DOI: 10.1002/ejic.201100157

DNA Cleavage by Structurally Characterized Dinuclear Copper(II) Complexes Based on Triazine

Salah S. Massoud,*[a] Febee R. Louka,[a] Wu Xu,[a] Richard S. Perkins,[a] Ramon Vicente,[b] Jörg H. Albering,[c] and Franz A. Mautner[d]

Keywords: Copper / Dinuclear complexes / Bridging ligands / Magnetic properties / DNA cleavage

The reaction of 2-chloro-4,6-bis(di-2-picolylamino)-1,3,5-triazine (bdpaT^{Cl}) with copper(II) perchlorate and copper(II) chloride afforded two dinuclear complexes [Cu_2(μ-bdpaT^{Cl})(μ-OH)$_2$(H_2O)$_{0.5}$(ClO_4)$_{0.5}$](ClO_4)$_{1.5}$·(H_2O)$_{1.5}$ (**1**) and [Cu_2(μ-bdpaT^{Cl})Cl_4]·2CH_3OH (**2**), respectively. These complexes were characterized by IR, UV/Vis, and EPR spectroscopy, single-crystal X-ray crystallography, and temperature dependence magnetic susceptibility measurements (2–300 K) as well as by electrochemical and molar conductivity measurements. In **1**, each of the three N-donor atoms of the binucleating bdpaT^{Cl} ligand coordinate to Cu^{II} ions, which are further bridged by two OH^- anions in a distorted five-coordinate geometry. In addition, each Cu^{II} ion forms a Cu–O semicoordinate bond with an aqua ligand or perchlorato anion. The Cu···Cu distance across the hydroxido bridges is 2.9698(11) Å. In **2**, the bdpaT^{Cl} ligand acts as bis-tridentate ligand connecting the two Cu^{II} ions, and the five-coordinate geometry around each copper center is achieved by two terminal chloro ligands. Magnetic measurements revealed strong antiferromagnetic coupling in **1** (J = –311.2 cm^{-1}) and very weak coupling in **2** (J = –2.4 cm^{-1}). DNA cleavage by these two complexes has been investigated (pH = 7.0, 37 °C). Although the bridged dihydroxido complex **1** did not show any detectable cleavage for DNA, significant cleavage was observed with the tetrachloro complex **2**. Under pseudo-Michaelis–Menten kinetic conditions, the kinetic parameters k_{cat} = 2.53 × 10^{-5} s^{-1} and K_M = 1.44 × 10^{-4} M were determined for **2**. The k_{cat} value corresponds to a 2.5 × 10^6 fold rate enhancement over noncatalyzed DNA. Electrophoretic experiments conducted in the presence and absence of oxidative scavengers DMSO, KI, and NaN_3, and radical promoter H_2O_2 provide evidence for the oxidative cleavage of DNA by hydroxy radicals and hydrogen peroxide species.

Introduction

The design and synthesis of dinuclear 3d metal complexes is an attractive topic because of the potential applications of these compounds as catalysts, oxidizing agents,[1–3] electrochemical catalysts for the oxidation of alcohol, ether, and water,[4–6] biocatalysts for the hydrolysis of phosphodiesters,[7–12] and for DNA and RNA cleavage[12–15] as well as to mimic the active sites in metalloproteins.[16–18] Dinuclear dioxido-bridged complexes of Mn, Fe, Cu, and Ni have been reported to activate C–H bonds in aliphatic and aromatic compounds and to promote oxygen insertion reactions (monooxygenase).[19–22] Another feature of these complexes is their use in the field of molecular magnetism.[23–26] In general, two strategies were used to assemble metal centers by the use of binucleating ligands[1,8–10,13,18] and/or by employing small ligands that have the capability of bridging the metal centers, such as halides, pseudohalides, hydroxides, oxides, and peroxides.[14,17,18,21–26] It has been pointed out that steric repulsion in the structural skeleton of bulky coligands often plays an important role in forming multinuclear complexes in the presence of small bridging ligands and this approach provided a successful pathway in the synthesis of a number μ-hydroxido and μ-oxido complexes.[14,17,18,21,23,27,28]

As alluded to above, one of the important properties of dinuclear metal(II) complexes is their increased efficiency in hydrolyzing phosphate esters and in cleavage reactions of DNA compared to the related mononuclear species.[12–15] Such bimetallic cooperativity has been observed in the hydrolysis of phosphate esters by dinuclear copper(II) and zinc(II) complexes.[12–15,29–32] For example, in the hydrolysis of phosphate monoester, a 50-fold enhancement in the rate of reaction was observed when two bis(benzimidazolyl)cop-

[a] Department of Chemistry, University of Louisiana at Lafayette, P. O. Box 44370, Lafayette, LA 70504, USA
Fax: +1-337-482-5676
E-mail: ssmassoud@louisiana.edu
[b] Department de Química Inorgànica, Universitat de Barcelona, Martí i Franquès 1–11, 08028 Barcelona, Spain
[c] Institut für Chemische Technologie von Materialien, Technische Universität Graz, Stremayrgasse 16, 8010 Graz, Austria
[d] Institut für Physikalische and Theoretische Chemie, Technische Universität Graz, 8010 Graz, Austria
Supporting information for this article is available on the WWW under http://dx.doi.org/10.1002/ejic.201100157.

per(II) units linked by a bridging 2-phenoxy-1,3-xylyl group were used compared to the corresponding monomer.[29] A dinuclear copper(II) complex with two 1,4,7-triazacyclononane (tacn) units and naphthalenyl spacer groups accelerates the cleavage of the RNA model ApA by a factor of about 10^5, which is about 520 times more reactive per metal center (pH = 6, 25 °C) than its monomeric analog.[30] The hydrolysis of the monoribonucleotide GpppG, a model compound for the 5′-cap of mRNA, by the dinuclear copper(II) complex derived from bis(tacn) where the two tacn rings are linked by *p*- or *m*-xylyl groups was about 100 times more rapid than the corresponding mononuclear complex.[31] Similarly, dinuclear zinc(II) complexes based on 1,4,7,11-tetraazacyclododecane linked by different spacer groups were shown to catalyze the cleavage of plasmid DNA by the synergisic effect of the two zinc ions, which are separated by about 4 Å.[32]

Dinuclear copper(II) coordination compounds constructed from organic building blocks with another bridging ligand (dicyanamide, squarate dianion, $C_4O_4^{2-}$, pyrazine, hydroxide, alkoxide, oxide) may lead to diverse magnetic coupling. When the intradimer $Cu^{II}\cdots Cu^{II}$ distances are ≥ 7 Å, as in pyrazine-, dicyanamido-, and μ-1,3-$C_4O_4^{2-}$-bridged complexes, weak antiferromagnetic compounds are produced ($|J| \approx 0$–10 cm^{-1}, where J is the exchange coupling constant) regardless the topological parameters and intermolecular distances between the Cu^{II} centers.[33] On the other hand, di-μ-hydroxido-, di-μ-alkoxido-, and di-μ-dioxido-bridged dinuclear Cu^{II} complexes where the intradimer $Cu^{II}\cdots Cu^{II}$ distances are ≤ 4 Å yield moderate to strong antiferro- and ferromagnetic coupling ($J \approx +170$ to -510 cm^{-1}).[23–26,34–36] The magnetic interactions in the latter class of complexes bridged by oxygen donors to give a Cu_2O_2 moiety have been found to have a linear dependence between the bridging angle of Cu–O–Cu, ϕ, and J.[26]

Herein we report the synthesis, structural, electrochemical, and spectral characterization of two new dinuclear copper(II) complexes: di-μ-hydroxido $[Cu_2(\mu\text{-bdpaT}^{Cl})(\mu\text{-OH})_2(H_2O)_{0.5}(ClO_4)_{0.5}](ClO_4)_{1.5}\cdot(H_2O)_{1.5}$ **(1)** and tetrachloro $[Cu_2(\mu\text{-bdpaT}^{Cl})Cl_4]\cdot 2CH_3OH$ (**2**), where bdpaT^{Cl} = 2-chloro-4,6-bis(di-2-picolylamino)-1,3,5-triazine, which acts as a binucleating bridging ligand (Scheme 1). The magnetic properties of these two complexes and their catalytic cleavage of DNA under the physiological conditions have also been investigated. The relationship between the structure of the di-μ-hydroxido complex **1** and its magnetic behavior was correlated to related compounds.

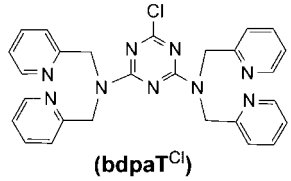

Scheme 1. Structural formula of 2-chloro-4,6-bis(di-2-picolylamino)-1,3,5-triazine.

Results and Discussion

Syntheses

2-Chloro-4,6-bis[bis(2-pyridylmethyl)amino]-1,3,5-triazine (bdpaT$^{Cl}\cdot 0.5H_2O$) was synthesized in good yield by reacting 2,4,6-trichloro-1,3,5-triazine with two equivalents of bis(2-pryidylmethyl)amine and diisopropylethylamine (DIPEA) in dry THF. The compound was characterized by ^{1}H and ^{13}C {H}NMR, and IR spectroscopy and by elemental analysis (see Exp. Section). Complexes **1** and **2** were synthesized in a straightforward manner. In methanolic solution, the reaction of bdpaT^{Cl} with two equimolar amounts of $Cu(ClO_4)_2\cdot 6H_2O$ afforded the navy blue complex $[Cu_2(bdpaT^{Cl})(OCH_3)_2](ClO_4)_2\cdot H_2O$ (**1a**), which was characterized by elemental analysis, spectroscopic, and molar conductivity measurements (see Exp. Section). Recrystallization of **1a** from H_2O produced the blue complex **1** in 63% yield.

When $CuCl_2\cdot H_2O$ was used instead of the perchlorate salt, the green complex **2** was obtained (93% yield). Complexes **1** and **2** were characterized by elemental analysis, IR, UV/Vis, and EPR spectroscopy, and single-crystal X-ray crystallography.

Characterization of the Complexes

The IR spectrum of **1** displays a strong band at around 3500 cm^{-1} that splits into two bands at 3434 and 3557 cm^{-1} characteristic of coordinated hydroxy groups and lattice water molecules, respectively. Similarly, a strong broad band centered around 3450 cm^{-1} was observed in **2** due to ν(O–H) of MeOH of crystallization. Complex **1** displays a very strong band at 1089 cm^{-1} attributed to the stretching ν(O–Cl) frequency of ClO_4^- ions. However, it should be mentioned that **1a**, which separated from the reaction of the methanolic solution of the ligand with copper(II) perchlorate was not the same as **1**. The methanolic product **1a** revealed a strong broad band at 3434 cm^{-1} due to lattice water and three strong perchlorate bands at 1120, 1105, and 1092 cm^{-1}. The splitting of the perchlorate band in the complex may result from a decrease in its symmetry to C_{3v} or to C_{2v}.

The visible spectroscopic data of **1** and **2**, recorded in H_2O and CH_3CN, and in MeOH for **2** reveal the presence of a broad d–d absorption band in the 600–900 nm region (see Exp. Section). In general, this feature is characteristic of five-coordinate copper(II) complexes of predominantly square pyramidal geometry (the broad band in the 600–700 nm range results from a $^2B_1 \leftarrow {}^2E$ transition), which is often associated with a low-energy shoulder at $\lambda > 800$ nm.[37] The visible spectra of **1** and **1a** in H_2O, CH_3CN, and/or MeOH were similar in the positions of their λ_{max} at the low-energy region; both display a relatively broad strong band at around 640 nm and a low intensity one at around 570 nm. These criteria reveal the same chromophore around the central Cu^{II} ions in the two complexes: CuN_3O_2. The molar conductivity, Λ_M, of **1a** measured in

acetonitrile where the complex retains its identity as indicated by its bluish-grey color, was found to be 233 $\Omega^{-1}\,cm^2\,mol^{-1}$. This value is consistent with 1:2 electrolytic behavior.[38] Therefore, **1a** may be formulated as $[Cu_2(\mu\text{-bdpaT}^{Cl})(\mu\text{-}OCH_3)_2](ClO_4)_2\cdot H_2O$ in a fashion that is similar to the corresponding structurally characterized bridged dihydroxido complex **1**.

The visible spectrum of **2** not only showed strong dependence on the solvent used, but dissolution was also accompanied by color change. The low-energy broad d–d band was shifted from 647 to 720 to 800 nm on going from MeOH to H_2O to CH_3CN, respectively. This finding in solution is most likely attributed to the partial solvolysis of the coordinated chloride ion(s) in the tetrachloro complex, as represented by Equation (1). This process is also associated with an increased distortion towards trigonal bipyramidal geometry (TBP).[37] The aqua product, $[Cu_2(\mu\text{-bdpaT}^{Cl})(H_2O)_nCl_{4-n}]^{n+}$, was found to be stable over a period of more than 24 h.

$$[Cu_2(\mu\text{-bdpaT}^{Cl})Cl_4] + n\ Solv \rightleftharpoons [Cu_2(\mu\text{-bdpaT}^{Cl})(Solv)_nCl_{4-n}]^{n+} + nCl^- \quad (1)$$

This result was supported by measuring the molar conductivity of the complex in aqueous solution to obtain a value of 364 $\Omega^{-1}\,cm^2\,mol^{-1}$, which corresponds to 1:3 electrolytic behavior[38] where the complex ion $[Cu_2(\mu\text{-bdpaT}^{Cl})(H_2O)_3Cl]^{3+}$ is the predominant species in H_2O.

X-band EPR spectra of **1** were measured for the solid sample and in DMF and CH_3CN solutions. Taking into account the dinuclear structure of **1**, which shows a strong antiferromagnetic coupling (J = –311.2 cm^{-1}) (see next section), we expect a low population of S = 1 at room temperature and a practically silent EPR spectrum. The recorded spectra show similar features with a wide range of broad weak signals except an intense narrow band located at g = 2.07, 2.10, and 2.09 for the solid sample, DMF, and CH_3CN solutions, respectively (Figure S1). This band could correspond to mononuclear Cu^{II} impurities. It is important to mention that the intensity of this narrow band did not increase in solution; if the dinuclear entity was broken in solution, then intensity of this band that is already present in the solid state as impurities should increase. The EPR spectrum of **1** measured after 24 h in DMF solution did not show spectral changes. These findings are not compatible with a simple mononuclear structure and most likely the dinuclear bridged dihydroxido structure is maintained as a solid and in solution. The room temperature X-band EPR spectra of **2** in the solid and in DMF/water are identical (Figure S2) indicating a mononuclear compound with $g_\perp$ = 2.12. Structurally the compound is dinuclear but magnetically the spectrum is the sum of two mononuclear species due to the long Cu1···Cu2 distance (7.2554 Å) and the negligible superexchange pathway (J = –2.4 cm^{-1}) provided by the bridging $bdpaT^{Cl}$ ligand.

Crystal Structure of 1

The crystal structure of **1** consists of dimeric cationic subunits, $[Cu_2(\mu\text{-bdpaT}^{Cl})(\mu\text{-OH})_2(ClO_4)_{0.5}(H_2O)_{0.5}]^{1.5+}$, and partially disordered ClO_4^- counter anions and lattice water molecules. A perspective view of the dimeric subunit is presented in Figure 1, and selected bond parameters are given in Table 1. In the dinuclear subunit the $bdpaT^{Cl}$ acts as a bis-tridentate ligand that connects two Cu^{II} centers, which are further bridged by two OH^- anions. The four coordination sites of each Cu^{II} center are occupied by O1 and O2 of the bridging hydroxido anions and two pyridyl N atoms of the $bdpaT^{Cl}$ ligand to form distorted square CuO_2N_2 planes with Cu–N/O bond lengths in the range 1.889(3)–2.015(4) Å. The acute interplanar angle formed by the two CuN_2O_2 planes is 14.2° and the intradimeric Cu1···Cu2 distance is 2.9808(9) Å. The hydroxido bridges form Cu1–O1–Cu2 and Cu1–O2–Cu2 bond angles of 100.18(3) and 103.02(13)°, respectively. The fifth coordination site of each Cu^{II} center is occupied by N3 and N9 amine atoms of the $bdpaT^{Cl}$ [Cu1–N3 2.638(4), Cu2–N9 2.619(4) Å]. Taking into account the half occupied O41 and O10 atoms of the disordered aqua ligand or perchlorato anion additional semicoordinative Cu–O interactions [Cu1–O41 2.580(5), Cu2–O10 2.867(5) Å] are present. Hydrogen bonds are listed in Table S1 (see Supporting Information).

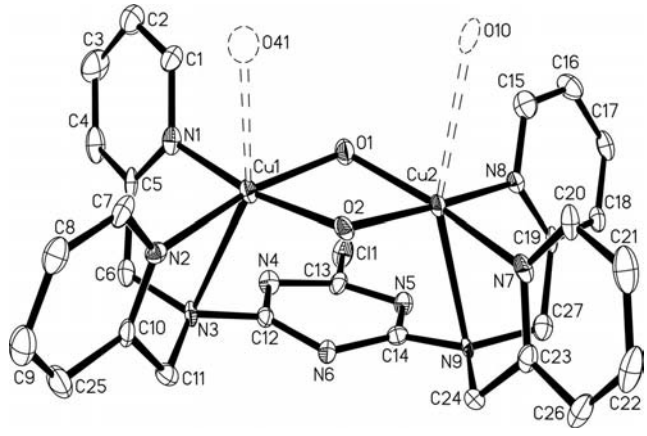

Figure 1. Perspective view of the dinuclear subunit of **1** showing the atom labeling scheme. Note: O10 of disordered ClO_4 anion and O41 of aqua ligand have an occupancy of 0.5.

Table 1. Selected bond lengths [Å] and angles [°] of **1**.

Cu1–O1	1.955(3)	Cu1–O2	1.889(3)
Cu1–N1	1.997(4)	Cu1–N2	2.015(4)
Cu1–N3	2.638(4)	Cu1–O41	2.580(5)
Cu2–O1	1.931(3)	Cu2–O2	1.919(3)
Cu2–N7	1.984(4)	Cu2–N8	2.003(4)
Cu2–N9	2.619(4)	Cu2–O10	2.867(5)
Cu1···Cu2	2.9808(9)		
O1–Cu1–O2	77.63(13)	O1–Cu1–N1	91.80(15)
O2–Cu1–N1	168.86(13)	O2–Cu1–N2	93.35(14)
N1–Cu1–N2	97.5(2)	N3–Cu1–O41	157.1(2)
O1–Cu2–O2	77.51(13)	O1–Cu2–N8	95.66(15)
O2–Cu2–N7	90.05(14)	O2–Cu2–N8	172.61(15)
N7–Cu2–N8	96.9(2)	N9–Cu2–O10	159.8(2)
Cu1–O1–Cu2	100.18(13)	Cu1–O2–Cu2	103.02(13)

Crystal Structure of 2

The crystal structure of **2** is formed by the neutral dinuclear complex $[Cu_2(\mu\text{-bdpaT}^{Cl})Cl_4]$ and partially disordered

MeOH solvent molecules. A perspective view of the dimeric subunit is given in Figure 2, and selected bond parameters are summarized in Table 2. As in **1**, the bdpaT^{Cl} acts as a bis-tridentate ligand to connect the two copper(II) centers, and the five-coordinate geometry around each copper center is completed by two terminal chloro ligands. The CuN_3Cl_2 chromophores may be described as between square planar and TBP geometry with τ values of 0.06 for Cu1 and 0.42 for Cu2.[39] The basal sites of each distorted copper polyhedron are occupied by two chloro ligands [Cu–Cl bond lengths vary from 2.247(2) to 2.314(2) Å] and two pyridyl N atoms of the bdpaT^{Cl} ligand [Cu–N_{py} bond lengths range from 1.972(5) to 2.034(5) Å]. The apical sites are occupied by N3 and N6 amine N atoms of the bdpaT^{Cl} ligand [Cu1–N3 2.613(5); Cu2–N9 2.390(4) Å]. The copper centers deviate from their basal CuN_2Cl_2 planes by 0.029 and 0.213 Å for Cu1 and Cu2, respectively. These CuN_2Cl_2 basal planes form interplanar angles of 40.2 and 25.7° for the Cu1 and Cu2 units, respectively, with the mean plane of the central C_3N_3 ring of the bridging bdpaT^{Cl} ligand. The intradimer Cu1···Cu2 distance is 7.2554(13) Å, and the shortest interdimeric Cu···Cu separation is 4.2519(11) Å. Hydrogen bonds are given in Table S1 and a packing diagram of **2** is given in Figure S3.

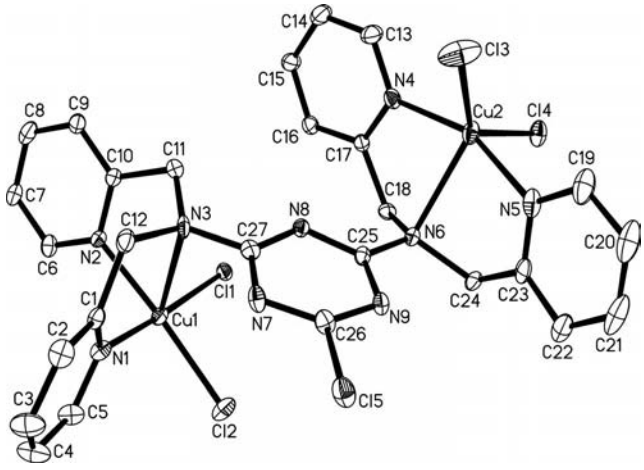

Figure 2. Perspective view of the dinuclear subunit of **2** together with the atom labeling scheme.

Table 2. Selected bond lengths [Å] and angles [°] of **2**.

Cu1–N1	2.018(4)	Cu1–N2	2.034(5)
Cu1–Cl1	2.261(2)	Cu1–Cl2	2.267(2)
Cu1–N3	2.613(5)	Cu2–N4	1.972(5)
Cu2–N5	1.988(5)	Cu2–Cl3	2.247(2)
Cu2–Cl4	2.314(2)	Cu2–N6	2.390(4)
N1–Cu1–N2	90.7(2)	N4–Cu2–N5	157.7(2)
N1–Cu1–Cl1	171.85(14)	N4–Cu2–Cl3	94.56(15)
N2–Cu1–Cl2	175.72(14)	N5–Cu2–Cl3	96.10(15)
N1–Cu1–Cl2	88.47(14)	N4–Cu2–Cl4	94.41(14)
Cl1–Cu1–Cl2	93.53(6)	N5–Cu2–Cl4	92.66(14)
N2–Cu1–Cl1	87.89(13)	Cl3–Cu2–Cl4	132.75(8)
N1–Cu1–N3	74.2(2)	N4–Cu2–N6	79.3(2)
N2–Cu1–N3	73.2(2)	N5–Cu2–N6	78.9(2)
N3–Cu1–Cl1	97.71(11)	N6–Cu2–Cl3	130.46(12)
N3–Cu1–Cl2	110.60(11)	N6–Cu2–Cl4	96.79(11)

Magnetic Properties

The magnetic behavior of **1** is shown in Figure 3 in the form of a plot of $\chi_M T$ vs. T. At 300 K, the $\chi_M T$ value is 0.42 $cm^3 K mol^{-1}$, which is clearly lower than that expected for two uncoupled $S = 1/2$ spins (0.75 $cm^3 K mol^{-1}$, $g = 2.0$), indicating strong antiferromagnetic coupling. Upon cooling, the $\chi_M T$ values decrease, arriving at zero at around 50 K. The χ_M vs. T plot for **1** shows a decrease on cooling from 13.9×10^{-4} $cm^3 mol^{-1}$ at 300 K to zero at around 50 K. For this compound, the χ_M vs. T plot increases on cooling from 50 K due to paramagnetic impurities. Based on this situation, the experimental magnetic data have been fitted using the Bleaney–Bowers expression based on the Hamiltonian $\hat{H} = -J\hat{S}_A \cdot \hat{S}_B$ with $S_A = S_B = 1/2$ including the presence of paramagnetic impurities [Equation (2)].

$$\chi_M = \{(2N g^2\mu_B{}^2/kT)[3 + \exp(-J/kT)]^{-1}\}(1 - \delta) + (N g^2\mu_B{}^2/4kT)(\delta) \quad (2)$$

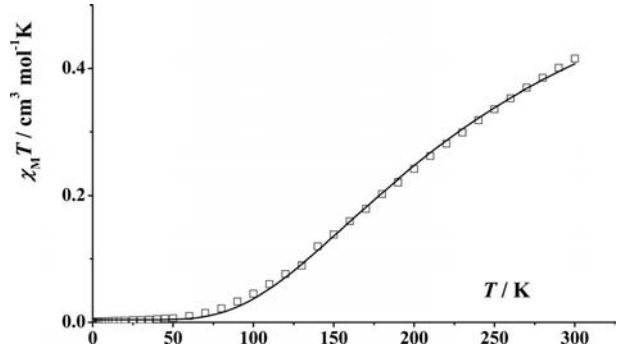

Figure 3. Temperature dependence of $\chi_M T$ of a solid sample of complex **1**. The solid line represents the best fit (see text).

The parameters N, μ_B and k in Equation (2) have their usual meanings, J = singlet–triplet splitting, and δ = molar fraction of noncoupled species. Least-squares fitting of all experimental data leads to the following parameters: $J = -311.2$ cm^{-1}, $g = 2.01$, and $\delta = 0.0114$. $R = \sum[(\chi_M T)_{obs} - (\chi_M T)_{calcd}]^2/\sum[(\chi_M T)_{obs}{}^2]$ inferior to $R = 1.0 \times 10^{-4}$.

The J value of **1** is in accordance with the expected value from the mean Cu–O–Cu bridging angle of $\phi = 101.8°$ by using the equation proposed by Crawford et al.:[26] $J = -74.53\ \phi + 7270$. The calculated J value of –317.1 cm^{-1} is in good agreement with the observed J value. In contrast, the relationship between the Cu–O–Cu bridging angles and experimental J values in the corresponding dinuclear Cu^{II} complexes containing bis(phenoxido) bridges was found to depend largely on the out-of-plane displacement of the phenyl groups.[40]

The magnetic behavior of compound **2**, illustrated in Figure 4, shows that at 300 K the $\chi_M T$ value is 0.88 $cm^3 K mol^{-1}$. This value is slightly higher than that expected for two uncoupled $S = 1/2$ spins (0.75 $cm^3 K mol^{-1}$, $g = 2.0$), indicating ferromagnetic coupling or $g > 2.0$. Upon cooling, the $\chi_M T$ values are practically constant, decreasing

from $T < 50$ K to a value of 0.54 $cm^3 K mol^{-1}$ at 2 K. The χ_M values increase on cooling from 2.5×10^{-3} $cm^3 mol^{-1}$ at 300 K without a maximum. This behavior indicates slight antiferromagnetic coupling. Based on this situation, the experimental magnetic data for **2** have been fitted using the Bleaney–Bowers expression based on the Hamiltonian $\hat{H} = -J\hat{S}_A \cdot \hat{S}_B$ with $S_A = S_B = 1/2$ [Equation (3)].

$$\chi_m = \{(2N\ g^2\mu_B^2/kT)[3 + \exp(-J/kT)]^{-1}\} \quad (3)$$

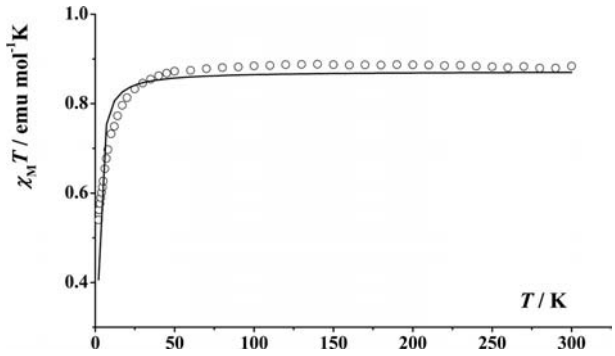

Figure 4. Temperature dependence of $\chi_M T$ of a solid sample of complex **2**. The solid line represents the best fit (see text).

Least-squares fitting of all experimental data led to the following parameters: $J = -2.4$ cm^{-1} and $g = 2.16$. The slight antiferromagnetic coupling can be understood by taking into account that the coordinating atoms of the bridging ligand, N(3) and N(6), occupy the apical positions of the coordination polyhedra of the copper atoms [Cu(1)–N(3) 2.612 Å, Cu(2)–N(6) 2.387 Å].

Electrochemistry

The cyclic voltammogram of **1** is shown in Figure S4 at a sweep rate of 100 mV/s. The curve begins at the open circuit potential of the system. There follows two complete anodic/cathodic sweeps and a final portion of cathodic sweep ending near the original open circuit potential. A noticeable difference was observed between the first and subsequent sweeps. For all the sweeps except the first there is a small but well defined cathodic peak at around 0.0 V and a broad region of cathodic reduction. On the anodic sweeps there are two well defined peaks though their size increases markedly from sweep to sweep. At higher sweep rates the anodic peak at around 0.0 V disappears and the other peaks change less from one sweep to the next.

Data were obtained that focused on the positive end (–0.310 V to +0.800 V) of the available potential range in DMF. Sweeps were performed from 100 to 3011 mV/s. Sweeps at all rates were similar except those at 500 mV/s and above. The cathodic and corresponding anodic peaks were obtained. The separation of the peaks and semiderivative analysis[41] indicate that the redox couple is irreversible. Mass transfer may also contribute to the complicated nature of the data. The complexity and irreversible nature of the redox couple preclude an accurate calculation of its formal potential but values of the intermediate potentials for the peaks in this range were calculated, found to be functions of sweep rate, and ranged from 0.30 to 0.34 V for the cyclic voltammetric and from 0.30 to 0.38 V for the semidifferential curves.

The cyclic voltammogram of **2** shows a large region of reduction followed by oxidation regions at around –0.3, 0.5, and 0.75 V. The oxidation peak at 0.75 V seen on the first sweep was anodic and assumed to be due to ligand oxidation. The rather weak anodic and cathodic signals more negative than 0.0 V may be due to minor ligand reactions and a second reduction of Cu^{II}. We focussed on the more prominent signals with shorter sweeps as shown in Figure 5, which contains three initial voltammetric segments. A well defined anodic peak is evident but there is only a broad region of reduction for which a peak potential cannot be measured. Reduction occurring in the first sweep segment beginning at 0.474 V was followed by an oxidation segment and another reduction. Several additional sweeps followed but are not included in Figure 5 for clarity.

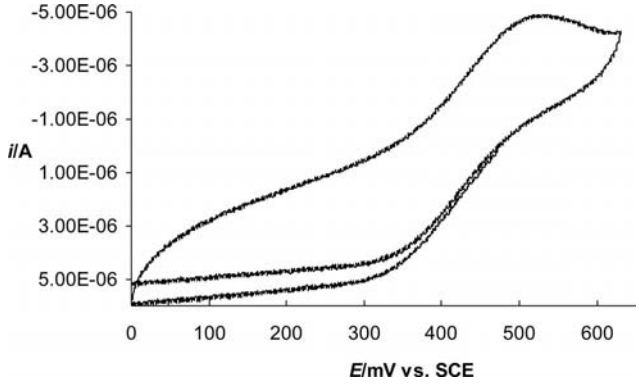

Figure 5. Cyclic voltammetric curve of **2** (1.0 mM) with $(C_2H_5)_4NClO_4$ (0.100 M) in DMF at a sweep rate of 200 mV/s.

Semiderivatives of the voltammogram segments (Figure 5) as well as those that followed were obtained. Similar plots were obtained at sweep rates ranging from 100 to 1505 mV/s. The semiderivative results show well defined peaks for both reduction and oxidation. From the E_{peak} values at these sweep rates it can be shown that the cathodic region and anodic peak in Figure 5 correspond to a quasi-reversible redox couple. If a one electron transfer is assumed then transfer coefficients of 0.45 and 0.49 are calculated for the cathodic and anodic reactions, respectively. The intermediate of the anodic and cathodic peak potentials on the semiderivative graphs ranged from 0.421 V to 0.428 V with an average of 0.425 V vs. SCE. These were taken as approximately the formal potential corresponding to a one electron reduction of Cu^{II}.

Cleavage of Plasmid DNA by 1 and 2

Although **1** did not exhibit any obvious DNA cleavage activity over a period of 24 h (Figure 6), the corresponding dinuclear tetrachloro complex **2** showed detectable DNA

cleavage where supercoiled DNA (form **I**) was cleaved to the relaxed open circular DNA (form **II**) as illustrated in Figure 7(a). The kinetics of DNA cleavage by **2** were measured by following the conversion of form **I** to form **II** at constant pUC19 DNA concentration (76.8 μM) and different complex **2** concentrations (50–450 μM) at different time intervals. The percentages of form **II** were plotted against time and the plots are shown in Figure 7(b). These plots followed a pseudo-first order kinetic profile and fit well to a single exponential curve using Equation (4) (see Exp. Section). From these curves, the cleavage rate constant, k_{obs}, at each concentration was calculated and the data are collected in Table 3. The values of the catalytic rate constant, k_{cat}, and the binding affinity constant, K_M, were evaluated from the linear plots of $1/k_{obs}$ vs. the reciprocal concentrations of the Cu^{II} complex, catalyst: [Cu complex], according to Equation (5). These experimental conditions allowed a pseudo-Michaelis–Menten analysis from which $k_{cat} = 2.53 \times 10^{-5}$ s^{-1} and $K_M = 1.44 \times 10^{-4}$ M were obtained. The calculated values of k_{cat} and K_M fall into the range reported for the cleavage of DNA by other metal complexes ($k_{cat} = 5.0 \times 10^{-5}$–$2.0 \times 10^{-4}$ s^{-1} and $K_M = 1.0 \times 10^{-4}$–2.0×10^{-3} M).[42–47]

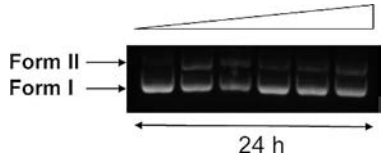

Figure 6. Electrophoretic separations of pUC19 plasmid DNA cleavage by **1**. Plasmid DNA (76.8 μM) was incubated with varying [**1**] (0, 50, 100, 150, 300, and 450 μM, from left to right lanes; molar ratio of [**1**]/[DNA] = 0, 0.651, 1.30, 1.95, 3.91, and 5.86, respectively) in 1.0 mM Tris-Cl buffer pH 7.0 for 24 h at 37 °C.

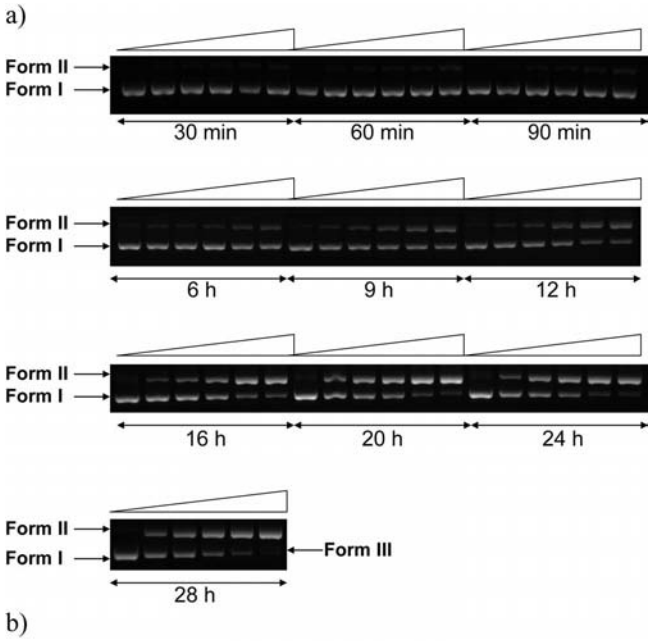

Figure 7. Cleavage profile of pUC19 plasmid DNA by **2**. (a) Forms **I**, **II**, and **III** as resolved by gel electrophoresis. DNA (76.8 μM) was incubated with varying concentrations of **2** (0, 50, 100, 150, 300, and 450 μM) in 1.0 mM Tris-Cl buffer pH 7.0 at 37 °C. (b) Quantified percentage of form **II** over the time.

[**2**] [μM]	k_{obs} [s^{-1}]	k_{cat} [s^{-1}]	K_M [M]
50	6.86×10^{-6}	2.53×10^{-5}	1.44×10^{-4}
100	9.29×10^{-6}		
150	1.15×10^{-5}		
300	1.67×10^{-5}		
450	2.70×10^{-5}		

Table 3. Pseudo-Michaelis–Menten kinetic data for the cleavage of pUC19 plasmid DNA (76.8 μM) at different concentrations of **2**.

In order to establish the DNA cleavage mechanism by **2** (oxidative mechanism vs. hydrolytic mechanism), the cleavage of DNA was further investigated in the presence and absence of scavengers of oxidative species. Oxidative cleavage of plasmid DNA species may lead to the formation of reactive singlet oxygen ($^1O_2$), hydrogen peroxide (H_2O_2), and/or hydroxy radical ($HO^{\cdot}$) species, which cause damage to the sugar and/or base.[48] To reveal the DNA cleavage mechanism by **2**, a singlet oxygen scavenger (NaN_3),[49] hydrogen peroxide scavenger (KI),[48,49] and hydroxy radical scavenger (DMSO) were used[49,50] and the results are illustrated in Figure 8. In two independent experiments for the cleavage of DNA by **2**, a decrease of percentage of form **II** was observed in the presence of DMSO (Figure 8, lane 4) and KI (Figure 8, lane 6) compared with the absence of DMSO and KI (Figure 8, lane 2). This demonstrates that hydroxy radicals and hydrogen peroxide are the active oxi-

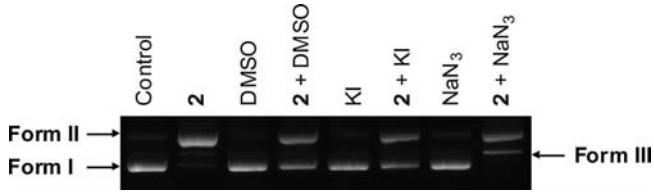

Figure 8. Electrophoretic separations of pUC19 plasmid DNA cleavage by **2** in the presence and absence of oxidative scavengers. Plasmid DNA (76.8 μM) was incubated with **2** (450 μM) in the presence of DMSO (0.4 M), KI (500 μM), and NaN_3 (500 μM) at 37 °C for 24 h.

dative species that promote the DNA cleavage by **2**. In addition, the DNA cleavage was dramatically enhanced in the presence of hydrogen peroxide (Figure S5), which again supports the increase of hydrogen peroxide catalytic activity.

Surprisingly, when NaN_3 was used a significant fraction of form **III** was observed (Figure 8, lane 8), suggesting that reactive singlet oxygen inhibits the DNA cleavage process. The DNA cleavage mechanism of form **II** to **III** by **2** in the presence of NaN_3 was further investigated by performing DNA ligation experiments of pUC19 plasmid DNA linearized by **2** in the presence of NaN_3 and by restriction enzyme *Eco*R I. Complex **2** cleaved pUC19 plasmid DNA into form **II** in the absence of NaN_3, but in the presence of NaN_3, form **II** was further cleaved to form **III**. The **2**-cleaved form **III** and linearized DNA by *Eco*R I migrated to the predicted positions (Figure 9). Both DNA bands were purified from the gel and the purified DNA was used in the ligation experiments. The appearance of high molecular weight bands indicates a successful ligation of *Eco*R I-linearized pUC19 by T4 DNA ligase. The observed fraction of one high molecular weight band after ligation in **2**-linearized pUC19 indicates that a hydrolytic mechanism is involved in the conversion of form **II** to **III** by **2** in the presence of NaN_3. The significant increase in the DNA cleavage activity by **2** in the presence of H_2O_2 and the inhibition of activity in the presence of DMSO and KI suggest that this reaction is preferentially proceeding by a hydroxy radical mechanism with $^{\cdot}OH$ and hydrogen peroxide species. The oxidative reaction pathway observed here has been suggested previously in the vast majority of DNA cleavage activity by copper complexes[14,15,48,51–56] and in the DNA photocleavage activity by some cobalt(III) complexes.[57]

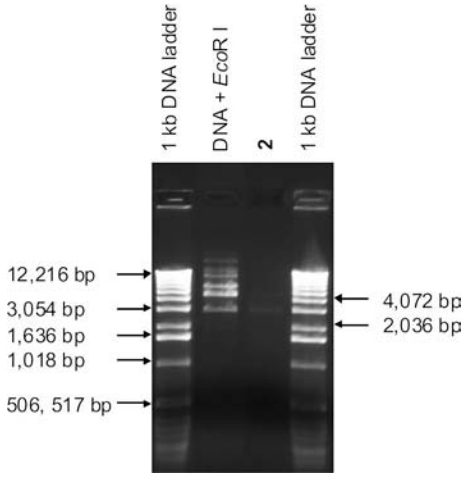

Figure 9. Gel electrophoresis for ligation of pUC19 plasmid DNA cleavage by **2** and by *Eco*R I. Lanes 1 and 4: 1 kb ladder (Invitrogen); lane 2: pUC19 linearized by *Eco*R I with T4 DNA ligase (Roche); lane 3: pUC19 linearized by **2** with T4 DNA ligase (Roche).

The rate enhancement for DNA cleavage by **2** or its hydrolytic active species $[Cu_2(\mu\text{-bdpaT}^{Cl})(H_2O)_3Cl]^{3+}$ corresponding to a 2.5×10^6 fold increase over the noncatalyzed DNA ($k = 1.0 \times 10^{-11}$ s^{-1} at 37 °C)[58] reveals the efficiency of this complex to cleave DNA. Comparable and even higher enhancements by copper(II) complexes have been reported for DNA cleavage when rates were compared at the saturation levels under pseudo-Michaelis–Menten kinetics.[46,47,51,55] Under similar physiological conditions, the trinuclear copper(II) complex $[Cu_3(TDAT)_2Cl_3]Cl_3{\cdot}2H_2O$ derived from 2,4,6-tris(di-2-pyridylamine)-1,3,5-triazine (TDAT) also exhibited efficient oxidative DNA cleavage.[56]

The lack of DNA cleavage activity by the bridged dihydroxido complex **1** does not seem to be unusual in light of the short Cu···Cu distance of 2.9808(9) Å in the bridging moiety of the $Cu(\mu\text{-}OH)_2Cu$ unit. The steric bulk induced by the planar triazine ring and the pyridyl groups around the Cu^{II} centers as well as the semicoordinative Cu–O bonds prevent the approach of the DNA to the metal centers. Similar results were reported for the hydrolysis of bis(4-nitrophenyl)phosphate (BNPP) by the monomeric Cu^{II}–tacn complex and its *N*-alkylated derivatives where the formation of the inactive dihydroxido-bridged dimeric species prevents BNPP hydrolysis.[59] In a related system derived from a dicopper(II) complex bridged by a hydroxy group and a phenolate oxygen atom, low catecholase-like activity was also observed.[14] In contrast to the lack of catalytic DNA cleavage by **1**, the doubly bridged dihydroxido–dicobalt(III) complexes constructed from tacn-*N*-acetate were found to be 40 times more reactive (under pseudo-Michaelis–Menten conditions $k_{cat} = 9.9 \times 10^{-4}$ s^{-1})[60] than **2**.

Conclusions

The findings reported here demonstrate that the nature of the copper(II) salt used in the synthesis of dinuclear copper(II) complexes of 2-chloro-4,6-bis(di-2-picolylamino)-1,3,5-triazine has a great influence on the structural, magnetic, and electrochemical properties of the resulting complex and hence their DNA cleavage activity. Although the tetrachloro complex **2** is a moderately efficient nuclease in promoting the DNA cleavage, a million fold over the noncatalyzed DNA, the corresponding bridging dihydroxido complex **1** is catalytically inactive. The short Cu···Cu distance in this complex is reflected by the strong magnetic coupling between the two copper(II) centers through the dihydroxido bridges in the complex and plays a crucial role in inhibiting its reactivity. From a structural point of view this was attributed to the steric environment imposed by the triazine ring which prevents the DNA from approaching the central copper(II) ions. Complex **2** is a promising candidate for DNA cleavage reactions. Increasing the catalytic activity of **2** by modifying the structural skeleton of the pendant pyridyl arms attached to the triazine ring and/or by substituting the triazine chloride group in the ligand by a bulky substituent is under investigation.

Experimental Section

Materials: The compounds bis(2-pyridylmethyl)amine (DPA) and 2,4,6-trichloro-1,3,5-triazine were purchased from TCI-America, and DIPEA was obtained from Aldrich Chem. Company, USA. All other chemicals were reagent grade quality.

Physical Measurements: Infrared spectra were recorded with a JASCO FT/IR-480 plus spectrometer as KBr pellets. Electronic spectra were recorded using an Agilent 8453 HP diode UV/Vis spectrophotometer. ^{1}H and ^{13}C NMR spectra were obtained at room temperature with a Varian 400 NMR spectrometer operating at 400 MHz (^{1}H) and 100 MHz (^{13}C). ^{1}H and ^{13}C NMR chemical shifts (δ) are reported in ppm and were referenced internally to residual solvent resonances, [D$_6$]DMSO: δ_H = 2.49, δ_C = 39.4 ppm. EPR measurements were performed for polycrystalline powder and in solution using DMF and/or CH_3CN. The spectra were recorded at room temperature with a Bruker ES200 spectrometer at X-band frequency (Magnetochemistry Service at the University of Barcelona). Molar conductance, Λ_M, of **2** was measured in H_2O at 25 °C with platinized platinum electrodes. A Wheatstone bridge circuit was used with a 1.00 kHz alternating current and the bridge balance was detected with an oscilloscope. The cell constant was calibrated with 0.0200 M KCl solution. Cyclic voltammetry was performed using a BAS CV-50 W voltammetric analyzer and a three-electrode cell with a Pt disk working electrode, a Pt wire counter electrode, and a saturated calomel reference electrode. Dry DMF was used as the solvent with tetraethyl ammonium perchlorate as the supporting electrolyte. Solutions were deaerated with Ar bubbling. Voltammograms were obtained under quiescent solution conditions. Magnetic susceptibility measurements under 1 T magnetic field in the range 2–300 K and magnetization measurements in the field range of 1–4 T were performed with a Quantum Design MPMS-XL SQUID magnetometer by the Magnetochemistry Service of the University of Barcelona. All measurements were performed with polycrystalline samples. Pascal's constants were used to estimate the diamagnetic corrections, which were subtracted from the experimental susceptibilities to give the corrected molar magnetic susceptibilities. pUC19 Plasmids were purified according to published procedures.[42] The plasmid DNA concentrations were determined spectrophotometrically by measuring their absorbance at 260 nm. Elemental analyses were carried out at the Atlantic Microlaboratory, Norcross, Georgia U.S.A.

Synthesis of the Ligand and Complexes

Caution! Perchlorate salts and their metal complexes are potentially explosive and should be handled with great care and in small quantities.

2-Chloro-4,6-bis[bis(2-pyridylmethyl)amino]-1,3,5-triazine (bdpaT^{Cl}·0.5H$_2$O): This compound was synthesized using a procedure similar to that described for the corresponding 2-chloro-4,6-bis[(dipyridin-2-yl-amino)]-1,3,5-triazine (CCDC-660712).[61] In a typical experiment, 2,4,6-trichloro-1,3,5-triazine (1.84 g, 10 mmol) and DIPEA (2.58 g, 20 mmol) were dissolved in dry THF (30 mL) in a two-necked round-bottom flask and the solution was cooled to 0 °C. While stirring this solution, one equivalent of DPA (2.00 g, 10 mmol) dissolved in THF (12 mL) was added dropwise over a period of 2 h. To the resulting yellowish-orange slurry, DPA (2.00 g, 10 mmol) dissolved in THF (12 mL) was added. The mixture was warmed to room temperature and then heated to reflux for 24 h under N_2. The solvent was removed at reduced pressure. The isolated crude solid was treated with CH_2Cl_2 (50 mL), filtered to remove diisopropylethylamine hydrochloride, and the solvents evaporated to dryness. The resulting product was recrystallized from MeOH with the aid of activated charcoal to afford the compound as an off-white solid (yield: 3.90 g, 75%); m.p. 138–140 °C, ^{1}H NMR ([D$_6$]CH_3COCH_3, 400 MHz): δ = 4.89, 5.03 (s, 2 H, CH_2); 7.24, 7.15 (dd, 2 H, 4-py-H); 7.06–7.08, 7.35–7.33 (d, 2 H, 6-py-H); 7.74–7.52 (dd, 2 H, 5-py-H); 8.50–8.42 (d, 2 H, 3-py-H) ppm. ^{13}C NMR ([D$_6$]CH_3COCH_3, 100 MHz): δ = 52.2, 52.1, 122.2, 121.4, 136.4, 149.2, 157.4, 166.0 ppm. Selected IR (KBr): $\tilde{\nu}$ = 3422 (w, br.), 1595 (s), 1573 (vs), 1507 (s), 1492 (vs) cm^{-1}. $C_{27}H_{25}N_9ClO_{0.5}$ (519.0): Calcd. C 62.89, H 4.83, N 24.06; found C 62.9, H 4.8, N 24.3.

[Cu$_2$(μ-bdpaT^{Cl})(μ-OH)$_2$(H$_2$O)$_{0.5}$(ClO$_4$)$_{0.5}$](ClO$_4$)$_{1.5}$·(H$_2$O)$_{1.5}$ (1): To a solution of the ligand (0.130 g, 0.25 mmol) in MeOH (20 mL) was added $Cu(ClO_4)_2$·6H_2O (0.190 g, 0.50 mmol) and the resulting bluish-green solution was heated on a steam bath for 5 min and then allowed to crystallize at room temperature. In the following day, the resulting navy-blue precipitate was collected by filtration, washed with Et_2O, and dried in air. The molecular formula of this complex was most likely consistent with [Cu$_2$(bdpaT^{Cl})(OCH)$_2$](ClO$_4$)$_2$·H_2O (**1a**) (yield: 72%). $C_{29}H_{32}Cl_3Cu_2N_9O_{11}$ (916.08): calcd. C 38.02, H 3.52, N, 13.76; found C 38.46, H 3.66, N 13.56. Λ_M (CH_3CN) = 233 Ω^{-1}cm^{2}mol^{-1}. Selected IR (KBr): $\tilde{\nu}$ = 3434 (s, br.), 1092, 1105, 1120 (vs, split) cm^{-1}. UV/Vis: λ_{max} (ε, M^{-1}cm^{-1}) in H_2O ≈ 508 (33), ≈ 567 (28), 636 (62); in MeOH ≈ 567 (15), 640 (80); in CH_3CN ≈ 510 (38), ≈ 570 (51), 638 (69).

Crystallization of **1a** from H_2O afforded **1** as blue single crystals, which were collected by filtration, washed with 2-propanol and ether, and air-dried (yield: 62%). $C_{27}H_{30}Cl_3Cu_2N_9O_{12}$ (906.04 g/mol): calcd. C 35.74, H 3.34, N 13.91; found C 36.18, H 3.34, N, 13.91. Selected IR (KBr): $\tilde{\nu}$ = 3557 (s, br.), 3434 (s, br.), 1089 (vs, centered) cm^{-1}. UV/Vis λ_{max} (ε, M^{-1}cm^{-1}) in H_2O = 355 (1470), 644 (53); in CH_3CN = 510 (sh), 570 (54), 638 (95).

[Cu$_2$(μ-bdpaT^{Cl})Cl$_4$]·2CH$_3$OH (2): Copper(II) chloride dihydrate (0.068 g, 0.500 mmol) was added to bdpaT^{Cl} (0.130 g, 0.25 mmol) dissolved in MeOH. The resulting bright green solution was heated for 5 min on a steam bath and allowed to crystallize at room temperature. The shiny green crystals that separated the following day were collected by filtration, washed with diethyl ether, and air-dried (overall yield: 0.196 g, 93%). $C_{29}H_{32}Cl_5Cu_2N_9O_2$ (842.99): calcd. C 41.32, H 3.83, N 14.95; found C 41.16, H 3.82, N 14.87. Λ_M (H_2O, 25 °C) = 364 Ω^{-1}cm^{2}mol^{-1}. Selected IR (KBr): 3450 (br. s, centered). UV/Vis: λ_{max} (ε, M^{-1}cm^{-1}) in MeOH = 510 (sh), 647; in H_2O: 480 (sh), ≈ 720 (br.); in CH_3CN = 465 (sh), ≈ 800 (br.).

X-ray Structure Determination: The X-ray single-crystal data for **1** and **2** were collected with a Bruker-AXS APEX II CCD diffractometer at 100(2) K. The crystallographic data, conditions retained for the intensity data collection, and some features of the structure refinements are listed in Table 4. The intensities were collected with Mo-K_α radiation (λ = 0.71073 Å). Data processing, Lorentz polarization and absorption corrections were performed using SAINT, APEX, and SADABS computer programs.[62,63] The structures were solved by direct methods and refined by full-matrix least-squares methods on F^2, using the SHELXTL program package.[64] All non-hydrogen atoms were refined anisotropically. The hydrogen atoms were located from difference Fourier maps assigned with isotropic displacement factors and included in the final refinement cycles on calculated positions. For **1**, a split occupancy of 0.5 was applied to disordered atoms of two ClO_4^- counter anions and the water molecules. SADI constraints were applied to fix the geometry of the disordered perchlorato ligands. For **2**, a split occupancy of 0.5 was applied to the two disordered CH_3OH solvent molecules.

Table 4. Crystallographic data for **1** and **2**.

	1	**2**
Empirical formula	$C_{54}H_{60}Cl_6Cu_4N_{18}O_{24}$	$C_{29}H_{32}Cl_5Cu_2N_9O_2$
Formula weight	1812.10	842.99
Crystal system	triclinic	monoclinic
Space group	$P\bar{1}$	$P2_1/c$
a /Å	11.8807(12)	10.8410(12)
b /Å	11.9556(12)	13.7665(13)
c /Å	13.6994(14)	24.186(2)
α /°	73.405(13)	90
β /°	84.853(14)	93.48(2)
γ /°	67.833(13)	90
V /Å^3	1726.6(4)	3602.9(6)
Z	1	4
μ /mm^{-1}	1.539	1.593
$\rho_{calcd.}$ /Mg m^{-3}	1.743	1.554
Crystal size /mm	0.34 × 0.27 × 0.19	0.28 × 0.21 × 0.13
Reflections collected	12259	25392
Reflections unique	6055	6335
Parameters	542	445
GOF	1.262	1.246
R_1, wR_2 (obsd. refl.)	0.0787, 0.1568	0.0651, 0.1677
R_1, wR_2 (all data)	0.0957, 0.1642	0.0742, 0.1717

CCDC-803720 (for **1**) and -803721 (for **2**) contain the supplementary crystallographic data for this paper. These data can be obtained free of charge from The Cambridge Crystallographic Data Centre via www.ccdc.cam.ac.uk/data_request/cif.

Plasmid DNA Cleavage by Copper(II) Complexes and Agarose Gel Electrophoresis: The procedures for plasmid DNA cleavage and gel electrophoresis were carried out as described elsewhere.[42] pUC19 Plasmid DNA (1 μg) was incubated with the Cu complexes at various concentrations in a total volume of 20 μL at 37 °C in a water bath for various incubation times. After incubation, bromophenol blue loading buffer was added. The samples were then loaded on a 1.0% agarose gel containing approximately 2.0 μg/mL ethidium bromide. Electrophoresis was carried out at 150 V for approximately 20 min in Tris-Borate-EDTA (TBE) buffer. The bands were visualized by UV light and photographed with a Bio-Rad gel documentation system. The % of the different plasmid DNA forms (**I**, **II**, and **III**) were quantified from the intensities of the corresponding forms using Quantity One software (Bio-Rad Laboratories, Hercules, CA 94547).

Kinetic Measurements for the DNA Cleavage by Copper(II) Complexes: DNA cleavage rates at varying concentrations of Cu complexes [0 (control), 50, 100, 150, 300, and 450 μM] were determined in 1.0 mM Tris-Cl buffer (pH = 7.0) at 37 °C for different intervals of time. The cleavage of DNA was fitted to a single-exponential curve (pseudo first-order kinetics)[55] using Origin 7.5 and Equation (4), where y_o is the initial percentage of a form of DNA and y is the percentage of the form of DNA at time t, to extract the hydrolysis rate constant, or apparent rate constant, k_{obs}.

$$y = (100 - y_o)[1 - \exp(-k_{obs}t)] \quad (4)$$

The values of k_{obs} were then plotted vs. the concentrations of copper(II) complexes [catalyst = copper(II) complex] [Equation (5)] allowing a pseudo-Michaelis–Menten analysis and the determination of the corresponding kinetic parameters:[55] hydrolysis rate constant, k_{cat}, and affinity constant, K_M.

$$k_{obs} = k_{cat}[\text{complex}]/(K_M + [\text{complex}]) \quad (5)$$

Supporting Information (see footnote on the first page of this article): Selected hydrogen bonds in the two complexes are included in Table S1. The EPR spectra of complexes **1** and **2**, the packing view of **2**, the cyclic voltammetry of **1**, and the electrophoretic separations of pUC19 plasmid DNA cleavage by **2** in the presence and absence of H_2O_2 or DMSO are shown in Figures S1–S5, respectively.

Acknowledgments

This research was financially supported by the Department of Chemistry, University of Louisiana at Lafayette. S. S. M. thanks Dean B. Clark (UL Lafayette), W. X. thanks the start-up fund from the College of Sciences (UL Lafayette), F. A. M. thanks Dr. J. Baumgartner (TU Graz) for assistance. Also, thanks go to two of the reviewers whose positive comments were helpful to improve the quality of the manuscript. R. V. acknowledges the financial support from the Spanish government project CTQ2009-07264 and the Generalitat of Catalunya project 2009SGR-1454.

[1] P. Gamez, P. de Hoog, M. Lutz, A. L. Spek, J. Reedijk, *Inorg. Chim. Acta* **2003**, *351*, 319.
[2] M. Ray, S. Mukerjee, R. N. Mukerjee, *J. Chem. Soc., Dalton Trans.* **1990**, 3635.
[3] K. Srinivasan, P. Michand, J. K. Kochi, *J. Am. Chem. Soc.* **1986**, *108*, 2309.
[4] P. A. Goodson, A. R. Oki, J. Glerup, D. J. Hodgson, *J. Am. Chem. Soc.* **1990**, *112*, 6248.
[5] R. Ramrai, A. Kira, M. Kaneko, *Angew. Chem.* **1986**, *98*, 824; *Angew. Chem. Int. Ed. Engl.* **1986**, *25*, 825.
[6] A. Gref, G. Balavoine, H. Riviere, C. P. Andrieux, *Nouv. J. Chim.* **1984**, *8*, 615.
[7] a) C. Liu, M. Wang, T. Zhang, H. Sun, *Coord. Chem. Rev.* **2004**, *248*, 147; b) P. Molenveld, J. F. J. Engbersen, D. N. Reinhoudt, *Chem. Soc. Rev.* **2000**, *29*, 75.
[8] M. Subat, K. Woinaroschy, C. Gerstal, B. Sarkar, W. Kaim, B. König, *Inorg. Chem.* **2008**, *47*, 4661.
[9] a) W. Y. Tsang, D. R. Edwards, C. T. Melnychuk, T. Liu, A. A. Neverov, N. H. Williams, R. S. Brown, *J. Am. Chem. Soc.* **2009**, *131*, 4159; b) S. E. Bunn, T. Liu, Z.-L. Lu, A. A. Neverov, R. S. Brown, *J. Am. Chem. Soc.* **2007**, *129*, 16238; c) Z.-L. Lu, T. Liu, A. A. Neverov, R. S. Brown, *J. Am. Chem. Soc.* **2007**, *129*, 11642.
[10] a) C. S. Rossiter, R. A. Mathews, I. M. A. Del Mundo, J. R. Morrow, *J. Inorg. Biochem.* **2009**, *103*, 64; b) C. S. Rossiter, R. A. Mathews, J. R. Morrow, *J. Inorg. Biochem.* **2007**, *101*, 925; c) A. O'Donoghue, S. Y. Pyun, M.-Y. Yang, J. R. Morrow, J. P. Richard, *J. Am. Chem. Soc.* **2006**, *128*, 1615.
[11] a) M. Wall, R. C. Hynes, J. Chin, *Angew. Chem. Int. Ed. Engl.***1993**, *32*, 1633; b) M. J. Young, J. Chin, *J. Am. Chem. Soc.* **1995**, *117*, 10577.
[12] L. M. Rossi, A. Neves, R. Hörner, H. Terenzi, B. Szpoganicz, J. Sugai, *Inorg. Chim. Acta* **2002**, *337*, 366.
[13] Y. Li, Y. Wu, J. Zhao, P. Yang, *J. Inorg. Biochem.* **2007**, *101*, 283.
[14] N. A. Rey, A. Neves, A. J. Bortoluzzi, C. T. Pich, H. Ternezi, *Inorg. Chem.* **2007**, *46*, 348.
[15] A. Arbuse, M. Font, M. A. Martinez, X. Fontrodona, M. J. Prieto, V. Moreno, X. Sala, A. Llobet, *Inorg. Chem.* **2009**, *48*, 11098.
[16] a) C. X. Zhang, H.-C. Liang, K. J. Humphreys, K. D. Karlin, in: *Catalysis by Metal Complexes*, vol. 26 (Eds.: R. Brian, R. James, W. N. M. Piet van Leeuwen), Kluwer Academic Publishers, Dordrecht, **2003**, chapter 2, p. 79–121; b) M.-A. Kopf, K. D. Karlin, in: *Biomimetic Oxidations* (Eds.: B. Meunier),

Imperial College Press, London, **2000**, chapter 7, p. 309–362; c) H.-C. Liang, M. Dahan, K. D. Karlin, *Current Opinion Chemical Biology* **1999**, *3*, 168; d) K. D. Karlin, A. D. Zuberbühler, in: *Bioinorganic Catalysis*, 2nd edition (Eds.: J. Reedijk, E. Bouwman), Marcel Dekker, New York, **1999**, chapter 14, p. 469–534.

[17] a) M. J. Henson, M. A. Vance, C. X. Zhang, H.-C. Liang, K. D. Karlin, E. I. Solomon, *J. Am. Chem. Soc.* **2003**, *125*, 5186; b) H. V. Obias, Y. Lin, N. N. Murthy, E. Pidcock, E. I. Solomon, M. Ralle, N. J. Blackburn, Y.-M. Neuhold, A. D. Zuberbühler, K. D. Karlin, *J. Am. Chem. Soc.* **1998**, *120*, 12960; c) D.-H. Lee, N. Wei, N. N. Murthy, Z. Tyeklár, K. D. Karlin, S. Kaderli, B. Jung, A. D. Zuberbühler, *J. Am. Chem. Soc.* **1995**, *117*, 12498.

[18] a) T. N. Sorrell, D. L. Jameson, C. J. O'Connor, *Inorg. Chem.* **1984**, *23*, 190; b) T. N. Sorrell, M. R. Malachowski, D. L. Jameson, *Inorg. Chem.* **1984**, *23*, 1250.

[19] a) D. Maiti, D. H. Lee, K. Gaoutchenova, C. Wurtele, M. C. Holthausen, A. A. N. Sarjeant, J. Sundermeyer, S. Schindler, K. D. Karlin, *Angew. Chem. Int. Ed.* **2008**, *47*, 82; b) L. Li, N. N. Murthy, J. Tesler, L. N. Zakharov, G. P. A. Yap, A. L. Rheingold, K. D. Karlin, S. Rokita, *Inorg. Chem.* **2006**, *45*, 7144.

[20] a) C. Kim, Y. Dong Jr., L. Que, *J. Am. Chem. Soc.* **1997**, *119*, 3635; b) J. A. Halfen, J. S. Mahapatra, E. C. Wilkinson, S. Kaderli, V. C. Yong Jr., L. Que, A. D. Zuberbuhler, W. B. Tolman, *Science* **1996**, *271*, 1397.

[21] a) Y. Gultneh, T. B. Yisgedu, Y. T. Tesema, R. J. Butcher, *Inorg. Chem.* **2003**, *42*, 1857; b) S. Itoh, H. Bandoh, S. Nagatomo, T. Kitagawa, S. Fukuzumi, *J. Am. Chem. Soc.* **1999**, *121*, 8945.

[22] a) S. V. Kryalov, E. V. Rybak-Akimova, *J. Chem. Soc., Dalton Trans.* **1999**, 3335; b) I. Blain, M. Giorgi, I. De Riggi, M. Réglier, *Eur. J. Inorg. Chem.* **2000**, 393.

[23] M. Arakawa-Itoh, K. Tokuman, Y. Mori, T. Kajiwara, Y. Fukuda, *Bull. Chem. Soc. Jpn.* **2009**, *82*, 358.

[24] a) E. Ruiz, P. Alemany, S. Alvarez, J. Cano, *J. Am. Chem. Soc.* **1997**, *119*, 1297; b) E. Ruiz, P. Alemany, S. Alvarez, J. Cano, *Inorg. Chem.* **1997**, *36*, 3683; c) S. Gehring, W. Hasse, *Mol. Cryst. Liq. Cryst.* **1989**, *176*, 513; d) H. Astheimer, W. Hasse, *J. Chem. Phys.* **1986**, *85*, 1427.

[25] H. Handa, N. Koga, S. Kida, *Bull. Chem. Soc. Jpn.* **1988**, *61*, 3853.

[26] V. H. Crawford, H. W. Richardson, J. R. Wasson, D. J. Hodgson, W. E. Hatfield, *Inorg. Chem.* **1976**, *15*, 2107.

[27] a) E. D. Estes, W. E. Hatfield, D. J. Hodgson, *Inorg. Chem.* **1974**, *13*, 1654; b) W. E. Hatfield, T. S. Piper, U. Klabunde, *Inorg. Chem.* **1963**, *2*, 629.

[28] a) C. Arcus, K. P. Fivizzani, S. F. Pavkovic, *J. Inorg. Nucl. Chem.* **1977**, *39*, 285; b) D. W. Meek, S. A. Ehrhardt, *Inorg. Chem.* **1965**, *4*, 584.

[29] W. Wall, R. C. Hynes, J. Chin, *Angew. Chem. Int. Ed. Engl.* **1993**, *32*, 1633.

[30] M. J. Young, J. Chin, *J. Am. Chem. Soc.* **1995**, *117*, 10577.

[31] a) K. P. McCue Jr., D. A. Voss Jr., C. Marks, J. R. Morrow, *J. Chem. Soc., Dalton Trans.* **1998**, 2961; b) K. P. McCue, J. R. Morrow, *Inorg. Chem.* **1999**, *38*, 6136.

[32] Q.-X. Xiang, J. Zhang, P.-Y. Liu, C.-Q. Xia, Z.-Y. Zhou, R.-G. Xie, X.-Q. Yu, *J. Inorg. Biochem.* **2005**, *99*, 1661.

[33] a) F. A. Mautner, J. H. Albering, M. Mikuriya, S. S. Massoud, *Inorg. Chem. Commun.* **2010**, *13*, 796; b) S. S. Massoud, P. J. Deifik, P. K. Bankole, R. Lalancette, G. Yee, D. Tatum, I. Bernal, F. A. Mautner, *Inorg. Chim. Acta* **2010**, *363*, 1001; c) T. LeGuet, F. A. Mautner, S. Demeshko, F. A. Meyer, R. S. Perkins, S. S. Massoud, *Inorg. Chem. Commun.* **2009**, *12*, 321; d) F. A. Mautner, M. Mikuriya, H. Ishida, F. R. Louka, J. W. Humphrey, S. S. Massoud, *Inorg. Chim. Acta* **2009**, *362*, 4073; e) S. S. Massoud, F. R. Louka, M. Mikuriya, H. Ishida, F. A. Mautner, *Inorg. Chem. Commun.* **2009**, *12*, 420; f) S. S. Massoud, F. A. Mautner, R. Vicente, F. R. Louka, *Eur. J. Inorg. Chem.* **2008**, 3709; g) S. S. Massoud, F. A. Mautner, R. Vicente, J. S. Dickens, *Inorg. Chim. Acta* **2008**, *361*, 299.

[34] a) J. A. Barnes, D. J. Hodgson, W. E. Hatfield, *Inorg. Chem.* **1972**, *11*, 144; b) D. Y. Jeter, D. L. Lewis, J. C. Hempel, D. J. Hodgson, W. E. Hatfield, *Inorg. Chem.* **1972**, *11*, 1958; c) D. L. Lewis, W. E. Hatfield, D. J. Hodgson, *Inorg. Chem.* **1972**, *11*, 2216; d) D. L. Lewis, K. T. McGregor, W. E. Hatfield, D. J. Hodgson, *Inorg. Chem.* **1974**, *13*, 1013; e) K. T. McGregor, N. T. Watkins, D. L. Lewis, R. F. Drake, D. J. Hodgson, W. E. Hatfield, *Inorg. Nucl. Chem. Lett.* **1973**, *9*, 423.

[35] a) M. Toofan, A. Boushehri, M. U. Haque, *J. Chem. Soc., Dalton Trans.* **1976**, 217; b) B. F. Hoskins, F. D. Whillans, *J. Chem. Soc., Dalton Trans.* **1975**, 1267.

[36] a) T. P. Mitchelle, W. H. Bernard, J. R. Wasson, *Acta Crystallogr., Sect. B* **1970**, *26*, 2096; b) B. J. Cole, W. H. Brumage, *J. Chem. Phys.* **1970**, *53*, 4718.

[37] a) B. J. Hathaway, in: G. Wilkinson, R. D. Gillard, J. A. McCleverty (Eds.), in: *Comprehensive Coordination Chemistry*, vol. 5, Pergamon, Press, Oxford, England, **1987**, p. 533; b) M. Duggan, N. Ray, B. J. Hathaway, G. Tomlinson, P. Brint, K. Pelin, *J. Chem. Soc., Dalton Trans.* **1980**, 1342.

[38] W. J. Geary, *Coord. Chem. Rev.* **1971**, *7*, 81.

[39] A. W. Addison, T. N. Rao, J. Reedijk, J. van Rijin, C. G. Verschoor, *J. Chem. Soc., Dalton Trans.* **1984**, 1349.

[40] D. Venegas-Yazigi, D. Aravena, E. Spodline, E. Ruiz, S. Alvarez, *Coord. Chem. Rev.* **2010**, *254*, 2086.

[41] P. Dalrymple-Alford, M. Goto, K. B. Oldham, *Anal. Chem.* **1977**, *49*, 1390.

[42] W. Xu, F. R. Louka, P. E. Doulain, C. A. Landry, F. A. Mautner, S. S. Massoud, *Polyhedron* **2009**, *28*, 1221.

[43] a) Y. An, M. L. Tong, L. N. Ji, Z. W. Mao, *Dalton Trans.* **2006**, 2066; b) Y. An, S.-D. Liu, S. Y. Deng, L.-N. Ji, Z. W. Mao, *J. Inorg. Biochem.* **2006**, *100*, 1586.

[44] J. Qian, W. Gu, H. Liu, F. Gao, L. Feng, S. Yan, D. Liao, P. Cheng, *Dalton Trans.* **2007**, 1060.

[45] M. Lanznaster, A. Neves, A. J. Bortoluzzi, V. V. Aires, B. Szpoganicz, H. Terenzi, P. C. Severino, J. M. Fuller, S. C. Drew, L. R. Gahan, G. R. Hanson, M. J. Riley, G. Schenk, *J. Biol. Inorg. Chem.* **2005**, *10*, 319.

[46] J.-L. Garcia-Giménez, G. Alzuet, M. González-Alvarez, A. Castiñeiras, M. Liu-González, J. Borrás, *Inorg. Chem.* **2007**, *46*, 7178.

[47] M. E. Branum, A. K. Tipton, S. Zhu Jr., L. Que, *J. Am. Chem. Soc.* **2001**, *123*, 1898.

[48] J.-T. Wang, Q. Xia, X.-H. Zheng, H.-Y. Chen, H. Chao, Z.-W. Mao, N. N. Ji, *Dalton Trans.* **2010**, *39*, 2128.

[49] X. Dong, X. Wang, M. Lin, H. Sun, X. Yang, Z. Guo, *Inorg. Chem.* **2010**, *49*, 2541.

[50] O. I. Aruoma, B. Halliwell, M. Dizdaroglu, *J. Biol. Chem.* **1989**, *264*, 13024.

[51] M. J. Fernandez, B. Wilson, M. Palacios, M. M. Rodrigo, K. B. Grant, A. Lorente, *Bioconjugate Chem.* **2007**, *18*, 121.

[52] a) S. Thyagarajan, N. N. Murty, A. A. Narducci Sarjeant, K. D. Karlin, S. E. Rokita, *J. Am. Chem. Soc.* **2006**, *128*, 7003; b) L. Q. Hatcher, K. D. Karlin, *J. Biol. Inorg. Chem.* **2004**, *9*, 669.

[53] L. M. Mirica, X. Ottenwaelder, D. P. Stack, *Chem. Rev.* **2004**, *104*, 1013.

[54] J. Hong, Y. Jiao, J. Yan, W. He, Z. Guo, L. Zhu, J. Zhang, *Inorg. Chim. Acta* **2010**, *363*, 793.

[55] A. Sreedhara, J. D. Freed, J. A. Cowan, *J. Am. Chem. Soc.* **2000**, *122*, 8814.

[56] J. Chen, X. Wang, Y. Shao, J. Zhu, Y. Zhu, Y. Li, Q. Xu, Z. Guo, *Inorg. Chem.* **2007**, *46*, 3306.

[57] a) R. Indumathy, T. Weyhermüller, B. U. Nair, *Dalton Trans.* **2010**, *39*, 2087; b) Y. Sun, Q.-X. Zhou, J.-R. Chen, Y.-J. Hou, W.-H. Lei, X.-S. Wang, B.-W. Zhang, *J. Inorg. Biochem.* **2009**, *103*, 1658.

[58] A. Radzicka, R. Wolfenden, *Science* **1995**, *267*, 90.

[59] a) E. L. Hegg, J. N. Burstyn, *Coord. Chem. Rev.* **1998**, *173*, 133; b) E. L. Hegg, S. H. Mortimore, C.-L. Cheung, J. E. Huyett, D. R. Powell, J. N. Burstyn, *Inorg. Chem.* **1999**, *38*, 2961; c) K. A. Deal, A. C. Hengge, J. N. Burstyn, *J. Am. Chem. Soc.* **1996**, *118*, 1713; d) K. A. Deal, J. N. Burstyn, *Inorg. Chem.* **1996**, *35*, 2792; e) K. M. Deck, T. A. Tseng, J. N. Burstyn, *Inorg. Chem.* **2002**, *41*, 669.
[60] J. Qian, X. Ma, J. Tian, W. Gu, J. Shang, X. Liu, S. Yan, *J. Inorg. Biochem.* **2010**, *104*, 993.
[61] P. de Hoog, P. Gamez, W. L. Driessen, J. Reedijk, *Tetrahedron Lett.* **2002**, *43*, 6783.
[62] Bruker (2005) SAINT v. 7.23; Bruker (2006) APEX 2, v. 2.0–2; Bruker AXS Inc. Madison, Wisconsin, USA.
[63] G. M. Sheldrick (**2001**), *SADABS v. 2*. University of Goettingen, Germany.
[64] G. M. Sheldrick, *Acta Crystallogr., Sect. A* **2008**, *64*, 112.
Received: February 17, 2011
Published Online: July 14, 2011

